Capabilities, Limitations and Challenges of Style Transfer with CycleGANs: A Study on Automatic Ring Design Generation

Tomas Cabezon Pedroso[1], Javier Del Ser[2,3], and Natalia Díaz-Rodríguez[4]

[1] Carnegie Mellon University, 5000 Forbes Ave., Pittsburgh, PA 15213, USA
[2] TECNALIA, Basque Research & Technology Alliance (BRTA), 48160 Derio, Spain
[3] University of the Basque Country (UPV/EHU), 48013 Bilbao, Spain
[4] Department of Computer Sciences and Artificial Intelligence, Andalusian Research Institute in Data Science and Computational Intelligence (DaSCI), CITIC, University of Granada, Granada, Spain
`tcabezon@andrew.cmu.edu, javier.delser@tecnalia.com, nataliadiaz@ugr.es`

Abstract. Rendering programs have changed the design process completely as they permit to see how the products will look before they are fabricated. However, the rendering process is complicated and takes a significant amount of time, not only in the rendering itself but in the setting of the scene as well. Materials, lights and cameras need to be set in order to get the best quality results. Nevertheless, the optimal output may not be obtained in the first render. This all makes the rendering process a tedious process. Since Goodfellow et al. introduced Generative Adversarial Networks (GANs) in 2014 [1], they have been used to generate computer-assigned synthetic data, from non-existing human faces to medical data analysis or image style transfer. GANs have been used to transfer image textures from one domain to another. However, paired data from both domains was needed. When Zhu et al. introduced the CycleGAN model, the elimination of this expensive constraint permitted transforming one image from one domain into another, without the need for paired data. This work validates the applicability of CycleGANs on style transfer from an initial sketch to a final render in 2D that represents a 3D design, a step that is paramount in every product design process. We inquiry the possibilities of including CycleGANs as part of the design pipeline, more precisely, applied to the rendering of ring designs. Our contribution entails a crucial part of the process as it allows the customer to see the final product before buying. This work sets a basis for future research, showing the possibilities of GANs in design and establishing a starting point for novel applications to approach crafts design.

Keywords: Deep Learning · Generative Adversarial Networks · Automatic Design · Image-to-image translation · Jewelry design · CycleGAN

1   Introduction

With the advances on artificial intelligence and deep learning (DL), the capabilities of computation in the field of design and computational creativity have spun. Machines have gone beyond doing what they are programmed to do, and debates spur questioning the creativity of models that, in any case, will not replace, but can definitely save time and assist designers do what they do best, more efficiently, and focusing on what really requires their expertise and skillful effort. Works in the intersection of design and computation are growing and are more relevant than ever. In the last years, engineers, researchers or artists have begun to explore the possibilities of artificial intelligence for creative tasks that can vary from the AI generated music of Arca that sounds in the MOMA's lobby[1] to the drawings by AARON computer program that can be visited at TATE Museum[2].

This work rises in this same intersection of design and technology, design and engineering, design and computation. The aim of this paper is to explore new areas and applications in which computers will change the way we consider design and the role that computers have on it. When this statement is made, often the fear of computers stealing people's jobs arises, nevertheless, this is not how we conceive this intersection of computers and design. While algorithms will spend time doing repetitive work, designers will be able to focus on what really matters: the users, the emotional feeling needs, innovations, or other needs... The objective is thus to make the most out of it for all agents taking part in the design process, from computer programs to designers. We believe the tools at our disposal cannot determine what we are capable of creating. Instead, AI, as another tool more, should serve to develop new ideas and not to limit the ones that the designer already has.

This work is organized in two parts, a theoretical one and a practical one, both complementary. The first one is motivated by the recent arrival of Generative Adversarial Networks (GAN) that since they were first introduced few years ago, in 2014 [5], have experimented and exponential growth and development. This research will be focus on the study and comprehension of the theory that supports GANs and their components. In the second part of the work, taking into account all of the above, a new tool of image generation is applied to an actual design problem, in this case, the rendering of an example of the XYU ring (finger, jewelry area). This tool will consist on a CycleGAN that taking as an input the sketch of the shape of the ring will generate a 3D object representation or a rendered image of it.

Although the steps in the design process can differ among authors, the whole process consists of going from a virtual concept or idea to the materialization in a concrete product[3]. This process starts with an initial brainstorming and,

---

[1] *Arca will use AI to soundtrack NYC's Museum of Modern Art*, https://www.engadget.com/2019-10-17-arca-ai-soundtrack-for-nyc-moma.html.

[2] *Untitled Computer Drawing*, by Harold Cohen, 1982, Tate. (n.d.), https://www.tate.org.uk/art/artworks/cohen-untitled-computer-drawing-t04167.

[3] *Design Thinking*, https://hbr.org/2008/06/design-thinking.

later, some of the concepts are developed, prototyped and, only after evaluation, the final product is selected. Computers have become fundamental in these last steps allowing designers not only to materialize their ideas with 3D objects and renders but also to show the clients how the final products look like. Actually, the famous furniture seller Ikea reaches their clients with the yearly catalogs, full of not real images but renderings of it[4]. Our ML model aims to input new tools for this last part of the design process.

While the proposed GANs have been used in a broad set of applications, we limit the scope of this paper to assess a potential technology impact that these models could have in automatic design. Although realistic images could be generated by other means, such as rendering, mocking up or photographing, in this work, the objective is not getting the output images themselves, but rather visually assessing the possibilities and limitations of paired GANs. More particularly, we will use GANs to assess the generative and creative capabilities to construct realistic and physically plausible designs. The concrete example we take is the rendering of a sketch of the XYU ring example. To approach this issue, we need to understand how GANs create images.

The rest of this paper is organized as follows. Section 2 briefly describes the state of the art on design tools and generative models for computational creativity with respect to design. Section 3 presents the proposed design model pipeline, Section 4 shows and examines critically the obtained results. Finally, Section 5 concludes with insights for further research and development.

2   Related work

A large body of works has emerged in the literature exploiting the highly performing abilities of generative models such as GANs. We briefly discuss those more closely related to automatic computational design generation.

With respect to neural rendering models, some approaches produce photo-realistic renderings given noisy or incomplete 3D or 2D observations. In Thies et al. [2], incomplete 3D inputs are processed to yield rich scene representations using neural textures, which regularize noisy measurements. Similar to our work, Sitzmann et al. [3] aggregate and encode geometry and appearance into a latent vector that is decoded using a differentiable ray marching algorithm. In contrast with our work, these methods either require 3D information during training, complicated rendering priors or expensive inference schemes. In [4] they present a way to learn neural scene representations directly from images, without 3D supervision, which permits to infer and render scenes in real time, while achieving comparable results to models requiring minutes for inference.

Since the introduction of generative adversarial networks (GANs) [1] and its spread use to generate data –from images to sound, music or even text–, a *zoo* of GANs has emerged. In the plethora of existing models we focus on style transfer

---

[4] *Why   IKEA   Uses   3D   Renders   vs.   Photography   for Their   Furniture   Catalog*,   https://www.cadcrowd.com/blog/ why-ikea-uses-3d-renders-vs-photography-for-their-furniture-catalog.

models that generally consist of translating images from one domain to a different one, where some dimension or data generating factor should be preserved. Style transfer was proposed by [5] as a neural algorithm able to disentangle content from style from an artistic image, and recombine these elements being taken from arbitrary images.

Among the most popular models for style transfer there are models that use paired datasets to perform image-to-image translation [6]. Image-to-image translation models can be used to generate street imaging from semantic segmentation masks (DCGAN [7], Pix2pixHD [8], DRPAN [9], SPADE [10], or OASIS [11]); however the need for paired data makes data collection tedious and costly.

When high-resolution photorealism is a priority despite the computational cost, models such as Pix2pixHD [8] have demonstrated to generate accurate images that are both physically-consistent and photorealistic (e.g., to visualize the impact of floods or ice melt [12,13]).

Alternative to GANs also exist to learn the distribution of possible image mappings more accurately [14], e.g., normalizing flows [15,16] or variational autoencoders [17], although they have shown this happens in detriment of the result realistic effect [18,19].

3   Proposed model for automatic ring design generation

In this section we present the motivating design problem and the model proposed to achieve this objective in an automatic manner.

3.1   Practical use case: designing XYU rings: traditional ring design pipeline

XYU is not only a ring but an algorithm to create rings[5][20]. This algorithm uses splines to generate infinite ring possibilities. The starting point is set by the user, who specifies the number of splines and the length and thickness of the ring. The control points of the splines are randomly selected and adapted to make them continuous on the ring. If the user does not like the result, the algorithm can be run again until an aesthetic shape is achieved.

The XYU ring algorithm allows the users to design their own 3D ring example based on their preferences, which are used by the algorithm to generate random rings. Each time the XYU ring code is run, a different and unique ring is produced. This procedure permits to personalize each of the XYU ring examples. Once the user finds a ring he/she likes, this is automatically modelled on *Maya* computer graphics application and the 3D object is sent to the jeweler. Each ring is 3D printed and cast, so each piece is unique.

The description of the actually used programs and different steps followed to go from the initial starting data to the final design of the ring are shown

---

[5] The XYU ring project is key to understanding this work. More information in https://tomascabezon.com/. XYU is the name of this project, it is not an acronym, but the name of this ring composed of 3 randomly chosen letters.
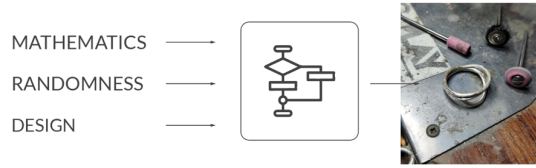
Fig. 1: Original conceptualisation schema for traditional ring design processes.
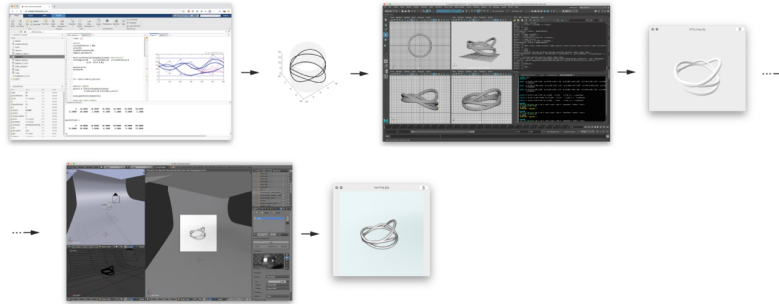

Fig. 2: Traditional pipeline and steps followed. On top Matlab program screenshot where the algorithm is run. In the middle, the Maya application with the 3D object of the ring. On the bottom, Blender software and the rendered image.

in Figure 2. The algorithm is run on Matlab, the ring is later automatically translated into Maya Embedded Language (MEL) language where the ring is 3D modelled and an .obj/.stl file is created. Finally, the realistic images of the ring are rendered using the Blender software.

To generate the 3D object and send the .obj file to the jeweler who will 3D print and cast it, *Maya 3D* application is used. To do so, the information of the ring is passed to Maya using the Maya MEL coding language. This is, the output of the Matlab algorithm is a .txt file with the instructions of the curves that generate the different brands of the ring, the splines, as well as the circumferences that will be extruded along the splines to form the 3D object. Therefore, the information to generate the ring in 3D is passed as coded instructions to Maya.

The last stage of the process corresponds to the rendering of the final product. In this last step, Blender rendering program is used to generate realistic images on the ring and to show the final product to the customer.

Rendering is the process of turning a 3D scene into a 2D image. A 3D scene is composed of various elements apart from the object we want to render, such as the background, the camera, the materials and the light. This step is the most tedious part of the XYU ring generation: the rendering of images not only takes a long time to be calculated, but scenes need to be arranged and the images do not always render as expected the first time. As a matter of fact, companies that create whole animation films by rendering each of the video frames of their films, such as Pixar, have rendering directors to optimize this process.
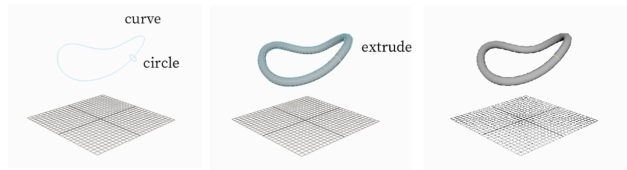
Fig. 3: Schema of how each of the brands of the ring are 3D modelled on Maya 3D modelling software. The points that compose the curve as well as the circle that will be extruded along this curve are passed to the Maya program using Maya MEL coding language.
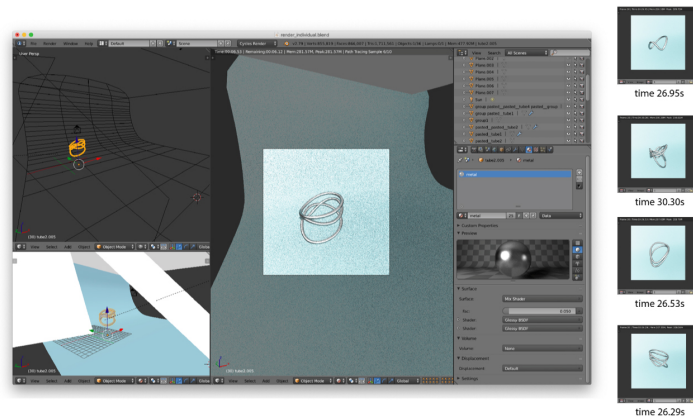

Fig. 4: Rendering settings and image rendering duration times for a set of 1000×1000 pixel size sample images.

To calculate how long it takes to render an image, on top of the time needed to compute the color of each pixel, which is not the longest one of the process, the scene setting time, the lighting configuration and the material generation and selection times should be added. A properly rendered image of an XYU ring would take, in total, around an hour in the making.

As it was seen, the original idea of completely automatizing the whole process of the XYU ring generation by the user was not achieved, as intermediate external programs need to be used in the process by the designer. Figure 6 shows the actual process intermediate steps needed for the 3D object generation and rendering.

3.2 Proposed Pipeline: Automatic design rendering through generative models for image-to-image translation

The initial process in which the generation of rings has been completely automatized has not been achieved yet. This limitation was the starting point that
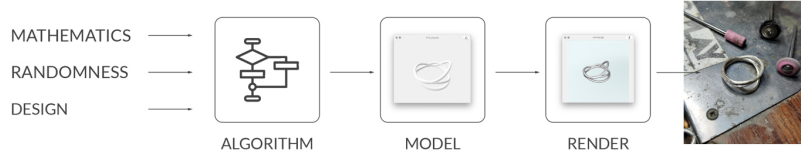
Fig. 5: Current traditional design pipeline schema from left to right: the algorithm run in Matlab, the 3D object modelled in Maya, rendered image in Blender and final product after being made by the jeweler. This process is slow and requires human intervention to render the 3D model.

motivates this work. Therefore, we propose a new approach for this ring design generation algorithm in which there is no need for the designer to be involved in the process of generating rendered images of the ring to show to the user.
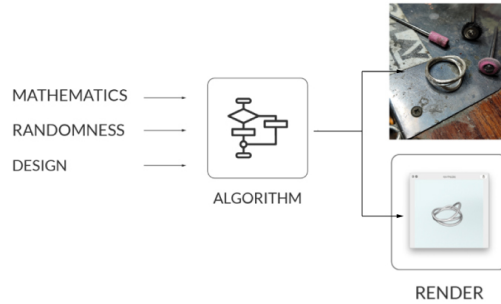

Fig. 6: Proposed model design pipeline. The algorithm generates not only the ring 3D object, but also its rendered images. The traditional rendering process is skipped, because it is automatically done by the CycleGAN within the full algorithm. The interesting aspect is that this allows: 1) the end user to instantaneously visualize the designed sample, which would not be possible without intervention from the designer to render it. 2) automating the full process.

It is important to note that the process for the jeweler does not change, as the 3D model file (e.g. .obj, .stl) is in both cases created for it to be 3D printed and later cast by the jeweler. This means the ring sketch is generated by the Matlab algorithm, which generates the different spline curves that compose the ring. These 3D spline curves are plotted in 2D and this image is used as input sketch for the CycleGAN. Therefore, since the algorithm also produces the rendering of the 3D models, the end user benefits from the CycleGAN by running it, choosing the preferred 3D model, and printing it in 3D, which means the full process is amenable to be automated.

3.3   CycleGAN as a generative model trained on unpaired images

CycleGANs [21] are generative models that are trained on unpaired sets of images in tuple format. They are used to translate between image *styles* or domains. Some examples can be seen in computer vision applications *translating* or transforming images from one domain into another (e.g. *horse2zebra*, *apple2orange*, *photo2Cezanne*, *winter2summer*... and vice versa).

In this work, we propose an innovative use of CycleGANs that consists of speeding up the last parts of the process of the design of XYU rings, i.e., their presentation. To achieve this, a *Sketch2Rendering* CycleGAN is trained. It will get a sketch image as an input and will apply a style transfer to generate a rendered image of the ring. In the following image this CycleGAN can be seen. Our hypothesis is that training a CycleGAN that would render the generated rings would not only ease this process and reduce its time but also automatize and speed up the process.
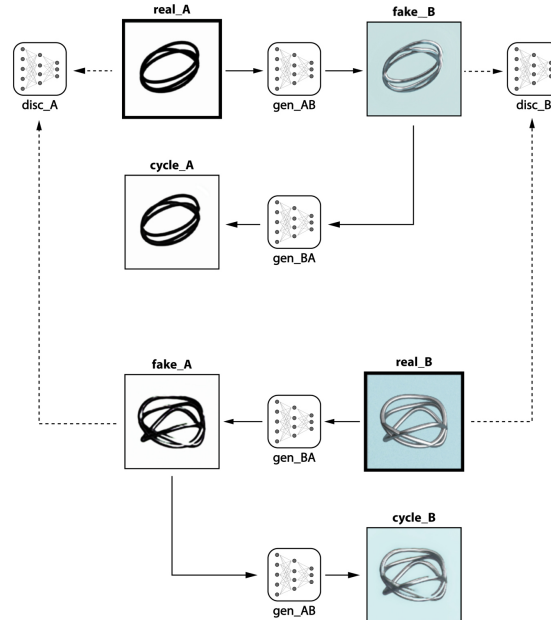
Fig. 7: Proposed CycleGAN where *gen* and *disc* prefixes stand for generator and discriminator, respectively. Input training images are the ones with a thicker frame.

One reason to choose CycleGANs against other *image2image* translation models is their ability to create infinite samples for a given input. The variational autoencoder (VAE) module that is part of the CycleGAN is responsible for this

feature, and one of the reasons behind our choice of this architecture. Against other models that are deterministic and thus, limited to produce a single unique output for a given input, a CycleGAN allows to produce a one-to-many output pairings for a given input image.

We propose a CycleGAN based on the one proposed by Zhu et al. as an unpaired Image-to-Image Translation using Cycle-Consistent Adversarial Networks [21]. The CycleGAN involves the automatic training of image-to-image translation models without paired examples. This capability is very suitable for this application, as there is no need for paired image datasets, since this is usually challenging and time consuming to obtain.

4   Results and analysis

In this section we present the produced designs by the CycleGAN architecture and provide some visual galleries to analyze them. Models, scripts and notebooks used to produce these results have been made publicly available[6].

4.1   *Sketch2Rendering* image results

In Figure 8 some examples of the style transfer performed by the once trained *Sketch2Rendering* CycleGAN are shown. For comparison purposes, some of the ring sketches used to train the data have been modelled and rendered using the traditional procedure. In the following image, the outputs of the CycleGAN are show next to what they could be some expected rendered images, using the *Maya* modelling program and *Blender* rendering program. Although the data consists of unpaired images, in Figure 8, images are show as pairs of the input sketch and the generated image by the Sketch2Rendering CycleGAN and the rendered image using Blender.

In Figures 9 and 10, 360 degrees of the same XYU ring can be seen. On the left, the input (sketch) image is shown and, next to it, an expected rendered image of the 3D object using Blender. On its right, the output of the *Sketch2Rendering* CycleGAN.

5   Discussion

After having shown the possibilities of the applications of style transfer with CycleGANs for rendering purposes, in this section, the artefacts found during the training and testing, as well as some of the limitations found on the model will be considered. Although the Sketch2Rendering model can achieve reasonable results in some cases, there are areas for improvement in future works. As it can be seen in the following lines, the results are far from uniformly positive and there are still some challenges and improvements to be done before good quality realistic images of rings are generated by the CycleGAN. The following describes some artefacts found both while training and testing the model.

---

[6] https://github.com/tcabezon/automatic-ring-design-generation-cycleGAN,
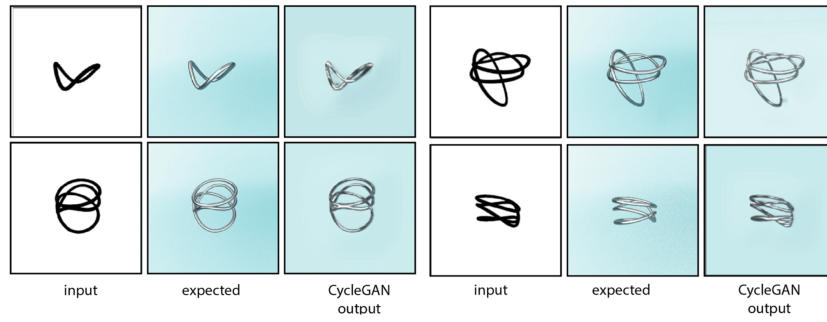https://tcabezon.github.io/automatic-ring-design-generation-cycleGAN/

Fig. 8: Different rings in the sketch domain and the rendered domain. The expected rendering were generated with Blender, while the other using the Sketch2Rendering CycleGAN.
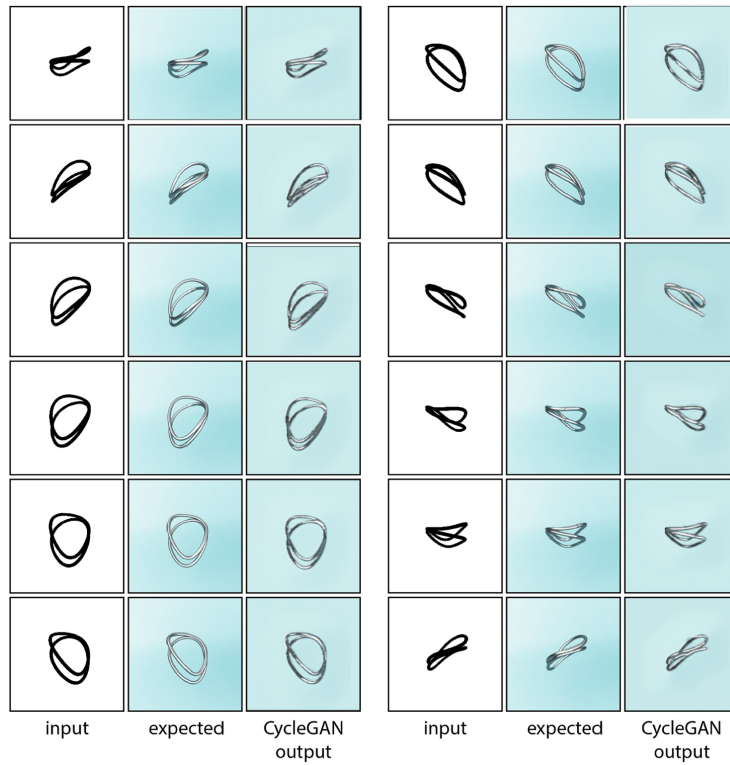

Fig. 9: Different views of the same object in the sketch domain and the rendered domain. The expected rendering was generated with Blender, while the other was generated by the Sketch2Rendering CycleGAN.
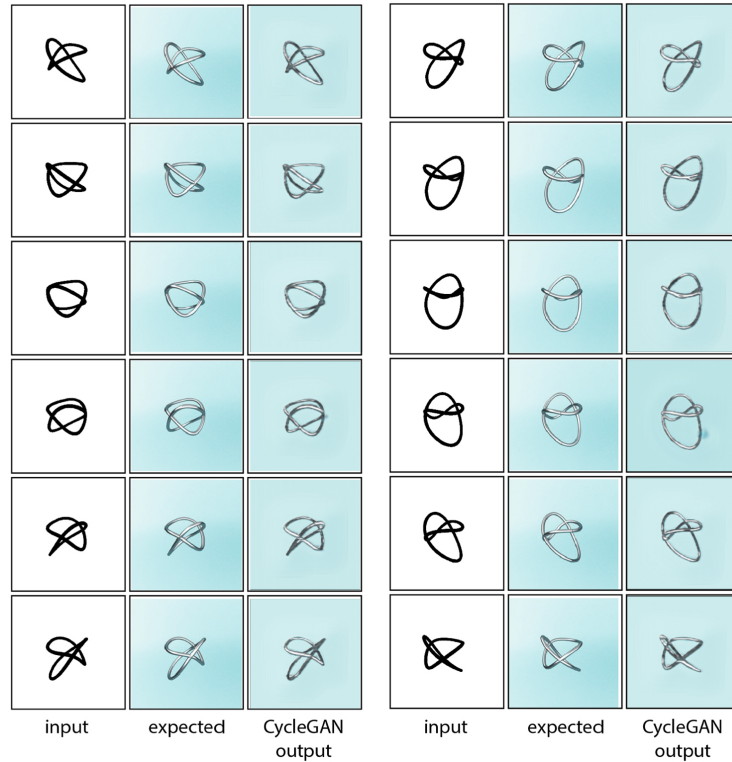
Fig. 10: Different views of the same object in the sketch domain and the rendered domain. The expected rendering was generated with Blender, while the one on the right of it was generated by the Sketch2Rendering CycleGAN.

5.1   Challenging aspects and detected artefacts

Appearance of white spots: During the training of the model, white blurry spots were found on the output images. These were usually found in the edge of the ring in areas where there is a strong shine on the ring, or where the different bands of the ring intersected.

***Aureoles* around the foreground object:** Exhibiting some kind of background *aureole* around the foreground object may be one of the most commonly found artefacts in the model outputs. The colour gradient or aureole shows around the edges of the ring. We could explain this effect to be due to the different lighting settings, since there is non uniform background color in the full training dataset. Actually, the rendered images created using the Blender program show noise in the background, as if a *Photoshop Film Grain* filter would have been applied to the background. This is due to the renderization parameters on Blender. In order to accelerate the renderization process, the number of

calculation steps for the color of each pixel was reduced when the dataset was created. In order to verify whether this is the actual cause of this artefact, in future works, better-quality datasets should be created, not only for the rings themselves but also for the backgrounds.

Checkerboard patterns: Checkerboard effect is a common and one of the most typical artefacts in GANs. The reason for this checkerboard-like pattern in images is due to the upsampling process of the images from the latent space, which becomes visible in images with strong colours. This artefact appears as a consequence of the ability of deconvolutions (i.e., transposed convolutions) to easily show an uneven overlap that adds *more of the metaphorical paint in some places than others* [22]. Since there are some solutions proposed for solving such artefact [22], these may be some of the first strategies to be applied in future works to improve the *pixelated*-looking effect on generated images.
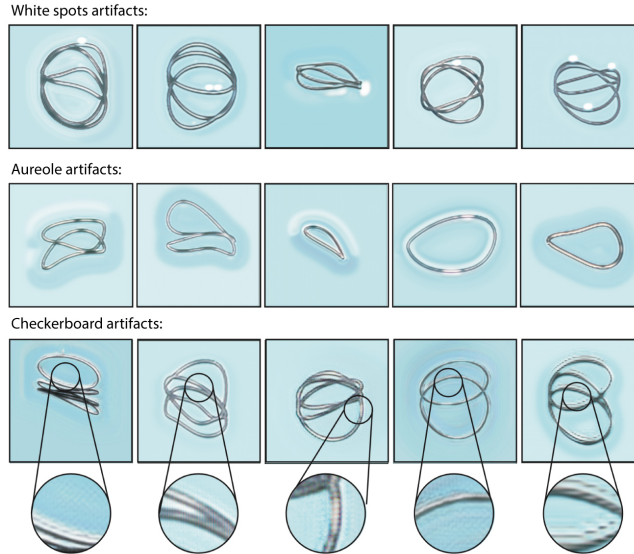

Fig. 11: Examples of generated samples by the Sketch2Rendering model exhibiting the different artefacts. Examples of the white spots artefact on the top, the aureole artefact in the middle, and the checkerboard pattern on the bottom.

5.2   Model limitations

Apart from the artefacts described in the previous section, some limitations of the actual model have been found. Solving these would require further development of the model itself, for example, using paired data for the lighting setting

to help guide the model to infer where the light comes from, or change how lines in the sketch intersect, for the model to better disentangle which one is on top of the other.

Coping with arbitrary lighting settings: In the following image, different lighting settings were used in the rendering of the same object with the same materials. Therefore, different images were created. Even if it may not be as realistic, in order to improve the training of the CycleGAN it could be beneficial for the model to be trained using always the same rendering settings, so that the CycleGAN is able to more sharply learn the rendering style.

Another solution, as previously mentioned, could be using other prior information or labeled data, e.g., adding information about the light position and direction, so the network can learn the differences. However, this would complicate the construction of datasets, since really precise information would be required to make sure that all the information about the lighting settings is included in the labels, which is something to be avoided, due to an increased cost in time and effort of the annotation process. Furthermore, this additional input would require some effective information fusion strategy for the model to leverage this information adequately.

Fig. 12: Examples of the influence of diverse lighting settings on the final renderings generated by the Sketch2Rendering model.

Learning to account for a 3D perspective: The sketch input image of the ring is an image of a 3D plot of the different splines that form the ring. Therefore, when in the 2D image two lines intersect, this may be because the lines actually intersect in the 3D space, or it may just be a consequence of the perspective. When creating a plot of a 3D object, some information is lost and thus, there is no way for the CycleGAN to know which of the intersecting lines in the image is on top of which or whether they are actually intersecting. A good way to solve this could be to use a different representation for intersecting lines and those that are not, for example, the diagrams used for knot representation in the study of mathematical knots [23] could be used. That way the model will learn when to render both of the splines together, or when they are not intersecting. In Figure 13 an example of this can be seen, on the top, the splines actually intersect; while in the bottom, both of the splines are separated.
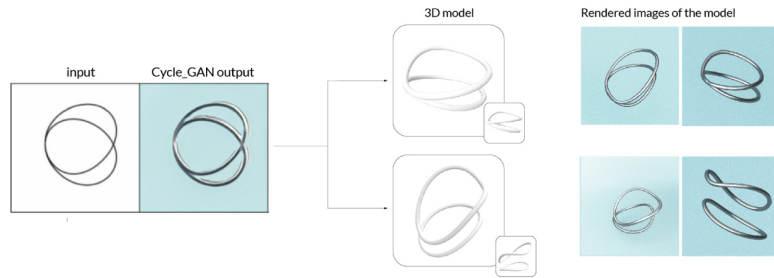
Fig. 13: Example of two lines intersecting in the 2D image, and two different 3D examples of the actually intersecting and non intersecting cases.

6   Conclusions and future work

After presenting the obtained results through the proposed and trained Cycle-GAN architecture and having discussed the problems encountered, some conclusions around the initially set objectives can be drawn.

First of all, we can assert that the Sketch2Rendering model can achieve compelling results for the rendering of the design through style transfer. That was the initial objective; nevertheless, as it was seen, there are areas for improvement in future works before high quality realistic images of the ring examples are generated by the CycleGAN. However, the results obtained exceed the initial expectations for this work. Indeed this new model supposes a new approach for the XYU ring algorithm and even though perfect results were not obtained, the reduction of the time and the allowance of a complete automation of the different ring design generation, makes this work an exemplary starting point for future research and improvements.

Secondly, this work shows the possibilities lying in the intersection of computation and design, which allows designers to focus on what really matters, while the algorithms do the repetitive non creative work. The rendering style transfer supposes going from the rendering of images that could take up to one hour on the making, to renders generated by the CycleGAN in seconds.

Therefore, it can be concluded that having developed a software that is capable of transferring the rendering style to the initial sketches of the ring, the research objective was achieved. The contribution of this work to the XYU ring design generation algorithm supposes an inflexion point for the way rings are shown to the end user, who now would be able to see real time rendered images of the ring that is being generated while interacting with the algorithm. Although we succeeded at the objective of validating image-to-image translation frameworks for automatic design rendering, some problems were encountered during the development of this work and discussed. We hope the research community finds the potential avenue of future works motivating for the exciting field of computational creativity and AI-assisted design to thrive.

In the future other types of GANs could be trained, e.g., models for higher resolution such as Pix2Pix, BiGAN or StyleGAN, and train them with paired data when available, to compare the gain in quality with this model's results. This quantitative comparison with other methods could help decide whether more dataset agnostic models that do not require paired data (such as the CycleGANs used in this work), are the best approach for this problem, or instead preparing paired data to train an image-to-image translation GAN is worth the time and effort. Future works should also assess some mathematical notions of correctness, and practical implications they could have for jewelry design.

Acknowledgments

References

1. Ian Goodfellow, Jean Pouget-Abadie, Mehdi Mirza, Bing Xu, David Warde-Farley, Sherjil Ozair, Aaron Courville, and Yoshua Bengio. Generative adversarial nets. *Advances in neural information processing systems*, 27, 2014.
2. Justus Thies, Michael Zollhöfer, Christian Theobalt, Marc Stamminger, and Matthias Nießner. Ignor: Image-guided neural object rendering. *arXiv preprint arXiv:1811.10720*, 2018.
3. Vincent Sitzmann, Justus Thies, Felix Heide, Matthias Nießner, Gordon Wetzstein, and Michael Zollhofer. Deepvoxels: Learning persistent 3d feature embeddings. In *Proceedings of the IEEE/CVF Conference on Computer Vision and Pattern Recognition*, pages 2437–2446, 2019.
4. Emilien Dupont, Bautista Miguel Angel, Alex Colburn, Aditya Sankar, Carlos Guestrin, Josh Susskind, and Qi Shan. Equivariant neural rendering. *arXiv preprint arXiv:2006.07630*, 2020.
5. Leon A Gatys, Alexander S Ecker, and Matthias Bethge. A neural algorithm of artistic style. *arXiv preprint arXiv:1508.06576*, 2015.
6. Phillip Isola, Jun-Yan Zhu, Tinghui Zhou, and Alexei A Efros. Image-to-image translation with conditional adversarial networks. In *Computer Vision and Pattern Recognition (CVPR), 2017 IEEE Conference on*, 2017.
7. Alec Radford, Luke Metz, and Soumith Chintala. Unsupervised representation learning with deep convolutional generative adversarial networks, 2016.
8. Ting-Chun Wang, Ming-Yu Liu, Jun-Yan Zhu, Andrew Tao, Jan Kautz, and Bryan Catanzaro. High-resolution image synthesis and semantic manipulation with conditional gans. In *Proceedings of the IEEE conference on computer vision and pattern recognition (CVPR)*, pages 8798–8807, 2018.
9. Chao Wang, Haiyong Zheng, Zhibin Yu, Ziqiang Zheng, Zhaorui Gu, and Bing Zheng. Discriminative region proposal adversarial networks for high-quality image-to-image translation. In *Proceedings of the European Conference on Computer Vision (ECCV)*, September 2018.

10. Taesung Park, Ming-Yu Liu, Ting-Chun Wang, and Jun-Yan Zhu. Semantic image synthesis with spatially-adaptive normalization. In *Proceedings of the IEEE Conference on Computer Vision and Pattern Recognition*, 2019.
11. Edgar Schönfeld, Vadim Sushko, Dan Zhang, Juergen Gall, Bernt Schiele, and Anna Khoreva. You only need adversarial supervision for semantic image synthesis. In *International Conference on Learning Representations*, 2021.
12. Björn Lütjens, Brandon Leshchinskiy, Christian Requena-Mesa, Farrukh Chishtie, Natalia Díaz-Rodríguez, Océane Boulais, Aruna Sankaranarayanan, Aaron Piña, Yarin Gal, Chedy Raïssi, et al. Physically-consistent generative adversarial networks for coastal flood visualization. *arXiv preprint arXiv:2104.04785*, 2021.
13. Björn Lütjens, Brandon Leshchinskiy, Christian Requena-Mesa, Farrukh Chishtie, Natalia Díaz-Rodriguez, Océane Boulais, Aaron Piña, Dava Newman, Alexander Lavin, Yarin Gal, et al. Physics-informed gans for coastal flood visualization. *arXiv preprint arXiv:2010.08103*, 2020.
14. Francesco Paolo Casale, Adrian Dalca, Luca Saglietti, Jennifer Listgarten, and Nicolo Fusi. Gaussian process prior variational autoencoders. In *Advances in Neural Information Processing Systems*, pages 10369–10380, 2018.
15. Danilo Rezende and Shakir Mohamed. Variational inference with normalizing flows. In Francis Bach and David Blei, editors, *Proceedings of the 32nd International Conference on Machine Learning (ICML)*, volume 37, pages 1530–1538, 2015.
16. Andreas Lugmayr, Martin Danelljan, Luc Van Gool, and Radu Timofte. Srflow: Learning the super-resolution space with normalizing flow. In *ECCV*, 2020.
17. Diederik P Kingma and Max Welling. Auto-encoding variational bayes. *Proceedings of the 2nd International Conference on Learning Representations (ICLR)*, 2014.
18. Alexey Dosovitskiy and Thomas Brox. Generating images with perceptual similarity metrics based on deep networks. In *Advances in Neural Information Processing Systems 29*, pages 658–666. Curran Associates, Inc., 2016.
19. Jun-Yan Zhu, Richard Zhang, Deepak Pathak, Trevor Darrell, Alexei A Efros, Oliver Wang, and Eli Shechtman. Toward multimodal image-to-image translation. In *Advances in Neural Information Processing Systems (NeurIPS) 30*, pages 465–476. 2017.
20. Tomas Cabezon Pedroso. Utilización de métodos aleatorios en la generación de formas geométricas. Master's thesis, Universidad Politécnica de Madrid, Spain. URL: https://oa.upm.es/69208/, 2003.
21. Jun-Yan Zhu, Taesung Park, Phillip Isola, and Alexei A Efros. Unpaired image-to-image translation using cycle-consistent adversarial networks. In *Computer Vision (ICCV), 2017 IEEE International Conference on*, 2017.
22. Augustus Odena, Vincent Dumoulin, and Chris Olah. Deconvolution and checkerboard artifacts. *Distill*, 1(10):e3, 2016.
23. Kunio Murasugi and Bohdan Kurpita. *Knot theory and its applications*. Springer, 1996.

A   APPENDIX: Supplementary materials

A.1   Datasets

Some randomly selected .jpg images from the different datasets generated for this work are shown in this section. The aim is to show the diversity of images that have been used for the purpose of training the CycleGAN.

Sketch2Rendering: 179 sketch images and 176 rendered images of the training dataset were used for the training. The images were scaled to 400 x 400 pixels when loaded. The Sketch dataset is composed of .jpg images. These, in Figure 14, have been generated using Matlab and the XYU ring algorithm. These images are a 3D plot of the splines that compose each of the rings, all with the same line thickness. The thickness was varied to show different ring thicknesses.

Rendered dataset: The images in Figure 14 have been created using the Blender rendering software. As it can be seen, although the background color has always been the same blue (#B9E2EA), the lighting setting has changed, as well as the camera position and orientation, and thus, different shadows and lights can be appreciated across the dataset.
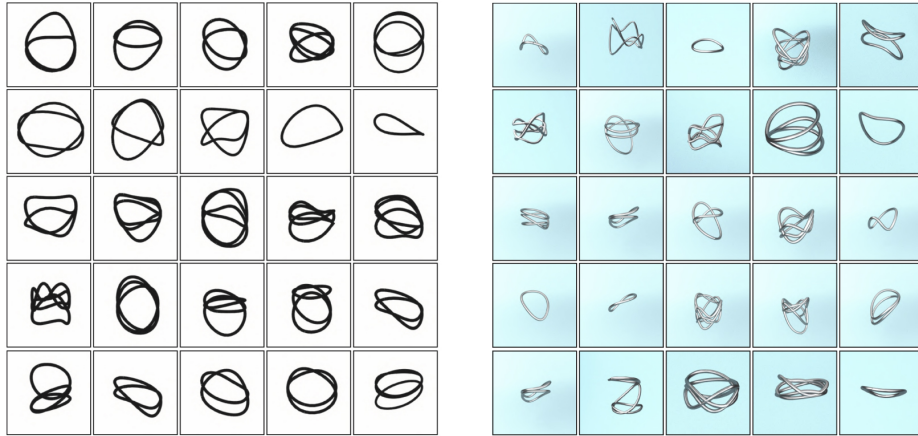

Fig. 14: On the left, random images of wire sketches created in Matlab language and used to train the CycleGAN model (domain A).On the right, random images of the rendered set of images, created using Blender rendering software, and used to train the CycleGAN model (domain B).

A.2   CycleGAN Model

To achieve a cycle consistency among two domains, a CycleGAN requires two generators: the fist generator (G_{AB}) will translate from domain A to B, and the second generator (G_{BA}) will translate from domain B back to A. Therefore, there will be two losses, one forward cycle consistency loss and other backward cycle consistency loss. These mean that $x* = G_{AB}(G_{BA}(x))$ and $y* = G_{BA}(G_{AB}(y))$.

CycleGAN Generator architecture: The generator in the CycleGAN has layers that implement three stages of computation:

1. The first stage encodes the input via a series of convolutional layers that extract image features.
2. the second stage then transforms the features by passing them through one or more residual blocks.
3. The third stage decodes the transformed features using a series of transposed convolutional layers, to build an output image of the same size as the input.

The residual block used in transformation stage 2 consists of a convolutional layer, where the input is added to the output of the convolution. This is done so that the characteristics of the output image (e.g., the shapes of objects) do not differ too much from the input. Figure 16 shows the proposed architecture with example paired images as input.

CycleGAN Discriminator architecture: The discriminator of the Cycle-GANs is based in the PatchGAN architecture [6]. The difference between this architecture and the usual GAN's discriminators is that the CycleGAN discriminator, instead of having a single float as an output, it outputs a matrix of values. A PatchGAN architecture will output a matrix of values, each of them between 0 (fake) and 1 (real), classifying the corresponding portions of the image.
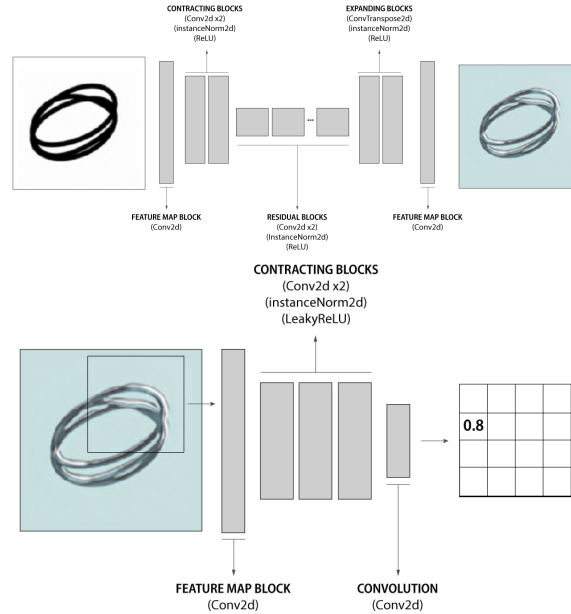

Fig. 15: Generator (upper) and Discriminator (below) architectures. Example classifying a portion of the image in the PatchGAN architecture, part of the CycleGAN discriminator. In this example 0.8 is the score the discriminator gave to that patch of the image (i.e., this patch looks closer to a real image (1)).
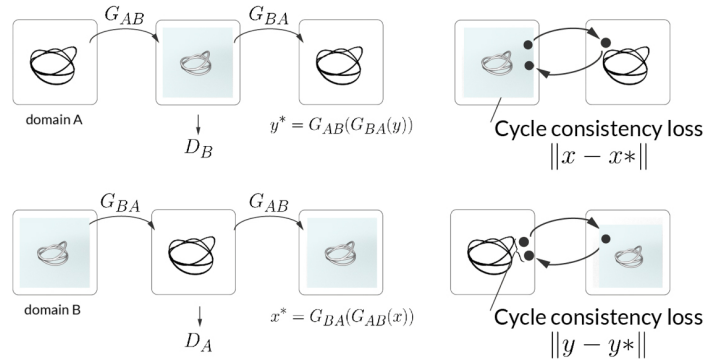
Fig. 16: Proposed CycleGAN model to learn an unsupervised Sketch2Rendering mapping.

Losses: The objective of CycleGANs is to learn the mapping between domains X and Y given training examples $x_i \in X$ and $y_i \in Y$. The data distributions are $x \sim p_{data}(x)$ and $y \sim p_{data}(y)$. As shown in Figure 16, the model includes two mappings, one learned by each generator, $G_{AB} : X \to Y$ and $G_{BA} : Y \to X$.

Apart from these generators, the model has two discriminators, one for each domain. D_X will learn to distinguish between real images x and fake images $x* = G_{BA}(y)$, while discriminator D_B will learn to distinguish between real images y and fake images $y* = G_{AB}(x)$. The objective functions will therefore contain two different losses, the adversarial losses [1] that will measure whether the distribution of the generated images match the data distribution in the target domain, and the cycle consistency losses [21], that will make sure that G_{AB} and G_{BA} do not contradict each other.

Cycle consistency loss: It can be expressed as $||x-x^*||$ or $||y-y^*||$, depending on which of the styles we consider as the starting point, where x^* and y^* represent the fake images generated by the generators. These equations ensure that the original image and the output image, after completing the cycle, i.e., the twice-translated image, are the same. This loss function is expressed as:

$$
\begin{aligned}
\mathcal{L}_{cyc}(G_{AB}, G_{BA}) = \ & \mathbb{E}_{x \sim p_{data}(x)}[||G_{BA}(G_{AB}(x)) - x||_1] \\
& + \mathbb{E}_{y \sim p_{data}(y)}[||G_{AB}(G_{BA}(y)) - y||_1]
\end{aligned} \tag{1}
$$

Adversarial loss: Apart from the cycle consistency loss, CycleGANs also use adversarial loss to train. As in traditional GAN models, the adversarial loss measures whether the generated images look real, i.e., whether they are indistinguishable from the ones coming from the same probability distribution learned

from the training set [1]. For the mapping $G_{AB} : X \rightarrow Y$ and the corresponding discriminator, we express the objective as:

$$
\begin{aligned}
\mathcal{L}_{GAN}(G_{AB}, D_B, X, Y) = \ & \mathbb{E}_{x \sim p_{data}(x)}[log D_B(y)] \\
& + \mathbb{E}_{x \sim p_{data}(x)}[log(1 - D_B(G_{AB}(x)))]
\end{aligned}
\tag{2}
$$

Every translation by the G_{AB} generator will be checked by the D_B discriminator, and the output of generator G_{BA} will be assessed and controlled by the D_A discriminator. Every time we translate from one domain to another, the discriminator will test if the output of the generator looks real or fake. Each generator will try to *fool* its adversary, the discriminator. While each generator tries to minimize the objective function, the corresponding discriminator tries to maximize it. The training objectives of this loss are $\min_{G_{AB}} \max_{D_B} \mathcal{L}_{GAN}(G_{AB}, D_B, X, Y)$ and $\min_{G_{BA}} \max_{D_A} \mathcal{L}_{GAN}(G_{BA}, D_A, X, Y)$.

Identity loss: The identity loss measures if the output of the CycleGAN preserves the overall color temperature or structure of the picture. Pixel distance is used to ensure that ideally there is no difference between the output and the input, this ensures that the CycleGAN only changes the parts of the image when it needs to.

Model training: The full objective of the CycleGAN is reducing these three loss functions. Actually, Zhu et al. show that training the networks with only one of the functions doesn't arrive to high-quality results. In the formula, we can see that both the identity loss and cycle consistency functions are weighted by λ_{ident} and λ_{cyc}, respectively. These scalars control the importance of each of the losses in the training. In our case, following the values for these parameters proposed in the original paper [21], λ_{cyc} will be 10, and λ_{ident} will be 0.1, as this last function only controls the tint of the background of the input and output images; and as our dataset is composed of the same colors, it does not suppose a large influence.

$$
\begin{aligned}
\mathcal{L}(G_{AB}, G_{BA}, D_A, D_B) = \ & \mathcal{L}_{GAN}(G_{AB}, D_B, X, Y) + \mathcal{L}_{GAN}(G_{BA}, D_A, X, Y) \\
& + \lambda_{cyc}\mathcal{L}_{cyc}(G_{AB}, G_{BA}) + \lambda_{ident}\mathcal{L}_{ident}(G_{AB}, G_{BA})
\end{aligned}
\tag{3}
$$

A.3   CycleGAN Training details

The networks were trained from scratch with a starting learning rate of 0.0002 for 100 epochs, after this, it was trained for 100 epochs more with a learning rate of 0.00002, as suggested by Zhu et. al in [21]. Following this procedure, the objective loss function of the discriminator D was divided by 2, which slows down the rate at which D learns compared with the generator G.

For the generator and discriminator we adopt the same architectures as the ones proposed by Zhu et al. [21], with the difference that for the first and last layers in the generator, we used a padding of 3 due to the input image size of our dataset.